

Determination of Kinetic Parameters and Applications of Measured Rate Law

Iodination of Acetone Reaction

Group 6 (Just Diene)

Group Leader: Daniel Robinson

Communication Coordinator: Abdul Fayed Abdul Kadir

Data Coordinator: Neel Shah

Safety and Logistics Coordinator: Evan Sciacchitano

May 16th, 2021

College of Engineering, Department of Chemical and Biomolecular Engineering
University of Delaware
Newark, Delaware 19711

Abstract

MATLAB P-Code is used to simulate various conditions for the iodination of acetone reaction by producing absorbance over time data. This data is directly correlated to the concentration of iodine over time which when used in combination with the varied initial conditions for each simulation, allowed for the determination of the rate orders for this reaction. The reaction orders were determined using ANOVA regression for the method of initial rates with rate order of acetone, hydrochloric acid, and iodine being 0.99 ± 0.02 , 1.00 ± 0.02 , and -0.0003 ± 0.0001 respectively. Rearranging the rate expression for this reaction, the rate constant could now be determined using the concentrations of each reagent with the rate of reaction. With the rate constant for each temperature now determined, the Arrhenius equation was used to determine the activation energy and pre-exponential factor, and it was found to be 83.01 ± 7.07 kJ·mol⁻¹ and $1.03 \times 10^{11} \pm 1.41 \times 10^{10}$ M⁻¹s⁻¹ respectively. To examine the autocatalytic nature of this reaction, MATLAB was further used to model the ordinary differential equations to represent the concentration profiles for each species of the reaction. The autocatalytic nature of this reaction offers potential problems for reaction runaway and so another model was simulated that incorporated hydrogen iodide electrolysis to reduce proton concentration, and therefore prevent reaction runaway. Analysis of the iodination of acetone reaction achieving 80% conversion of acetone in a continuously stirred tank reactor requires a reactor volume of 56.6 ± 4.9 L.

Table Of Contents

Abstract	1
List Of Tables	3
List Of Figures	3
1. Introduction	4
2. Experimental Method	5
2.1. Apparatus	5
2.2. Materials	5
2.3. Safety Hazards	5
2.4. Procedure	6
3. Results And Discussion	7
3.1. Determination of Reactions Orders α , β , and γ	7
3.2. Determination of Arrhenius Parameters A and Ea	7
3.3. Uncertainty Analyses	8
4. Application Of Rate Law	11
4.1. Analysis of the Autocatalytic Regime in BSTR	11
4.2. Analysis of Acetone Iodination in Conjunction with HI electrolysis	13
4.3. CSTR Sizing	15
5. Conclusions And Recommendations	16
5.1. Conclusions	16
5.2. Recommendations	16
6. Nomenclature Table	17
7. References	18
8. Appendices	18
Appendix A: Chemical Properties And Safety Hazards	18
Appendix B: Sample Calculations	19
Appendix C: Supplemental Sensitivity Analysis Discussion	21
Appendix D: MATLAB Code and Excel Sheet	23

List Of Tables

- Table 1:** Initial conditions of different runs for data simulations.
Table 2: Rate orders with respect to each reactant with associated errors and p-values.
Table 3: Arrhenius parameters from the predetermined rate orders.
Table 4: Determined parameters with their respective errors.
Table 5: Initial conditions to model autocatalytic behavior in BSTR.
Table 6: Initial conditions for the CSTR sizing.
Table 7: Final prediction of concentration and CSTR volume sizing.
Table 8: Summary of nomenclatures and abbreviations used throughout the report.
Table A1: Summary of safety hazards and protective measures of the reactants/products involved.
Table B1: Initial rate of reaction for each run from linear fitting of the I_2 concentration profile.
Table B2: MLR outputs to determine rate order with respect to each reactant.
Table B3: Variations in rate constants for Arrhenius parameters determination.

List Of Figures

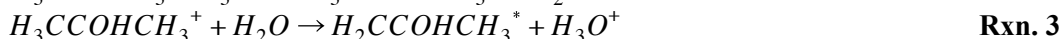
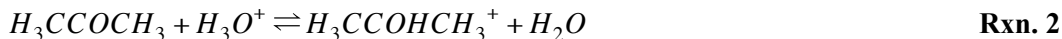
- Figure 1:** Schematic diagram of the experimental setup.
Figure 2: 95% confidence interval band for Arrhenius equation linearization for Run 11 - 14 data points.
Figure 3: Predicted data of acetone concentration in a batch reactor.
Figure 4: Predicted data of proton concentration in a batch reactor.
Figure 5: Predicted and simulated data of I_2 concentration in a batch reactor.
Figure 6: Predicted data of acetone concentration in a batch reactor with HI electrolysis.
Figure 7: Predicted data of proton concentration in a batch reactor with HI electrolysis.
Figure 8: Predicted and simulated data of I_2 concentration in a batch reactor with HI electrolysis.
Figure B1: Absorbance data varying with time for all run conditions.
Figure B2: a) Concentration of I_2 varying with time (left) and b) linear fitting for initial rate of reaction determination (right) for each run.
Figure C1: Changes in volume of CSTR after varying the predicted parameters from Phase 1 and 2.
Figure C2: Changes in volume of CSTR after varying the provided initial parameters from Phase 3.

1. Introduction

The determination of reaction rates is highly significant for the modeling of a reactor. A chemical reaction rate order dictates the rate at which a reaction proceeds, allowing one to determine a reactant conversion target as well as the potential of a runaway reaction. In this experiment, the chemical reaction in question is that of the iodination of acetone as shown in **Rxn. 1** shown below.



The overall reaction can be broken down into its elementary steps, as shown in **Rxn. 2 - 4**, from which the overall rate expression can be derived by rearranging the rate expression from these steps.



Rxn. 2 is the protonation of acetone, which is a relatively fast reaction and reaches pseudo equilibrium prior to the subsequent steps. In **Rxn. 3**, the protonated ketone undergoes rearrangement to make an enol and is stated as the rate determining step. Finally, the enol reacts with iodine and generates acetone and hydrogen iodide in **Rxn. 4**.

In the first part of this experiment, the rate law and Arrhenius parameters for this reaction were determined. The rate of reaction depends on the concentrations of different chemical species. Note that the reaction orders are not always equal to the respective stoichiometric coefficients, and must be determined experimentally. The rate law of the reaction can be generalized as shown in **Eq. 1**.

$$Rate = k[Acetone]^\alpha [HCl]^\beta [I_2]^\gamma \quad \text{Eq. 1}$$

From the analysis of elementary reactions, it was found that α , β , and γ take on the values of 1, 1, and 0, respectively. This means that the concentration gradient of iodine is linear with time, which can be studied using the initial rates method. To study the temperature dependence, the Arrhenius equation should be used, as shown in **Eq. 2**.

$$k = A \exp\left(-\frac{E_a}{RT}\right) \quad \text{Eq. 2}$$

The temperature and concentration can be measured; however, the reaction orders, activation energy, and Arrhenius constant must be determined experimentally. This reaction was chosen due to the ability to determine progress through the absorbance of UV light by iodine using a spectrophotometer. Using the Beer-Lambert law, as shown in **Eq. 3**, the absorbance values can be correlated to concentration.

$$A = \epsilon b[i] \quad \text{Eq. 3}$$

In the second part of this study, a batch reactor and continuous stirred reactor, CSTR, are modeled using the previously acquired kinetic parameters. It has been proposed that the reaction is first order with respect to acetone and hydrochloric acid, and zero order with respect to iodine indicating that the concentration of iodine has no impact on rate. The proposed rate law must be verified, and from the verification of this rate law, experiments with varying temperature can be used to determine the frequency factor and activation energy.

2. Experimental Method

2.1. Apparatus

Due to circumstances out of control, there was no physical setup of this lab. Instead, a MATLAB pseudo-code simulated data outputs resembling the data the physical apparatus would return had this been able to be completed in person. The MATLAB code is intended to accurately simulate the data outputs produced by the typical experimental method. This means it will have values of error and variability that must be considered in further analysis. Had this been done on purpose, it would be necessary to have a thorough understanding of the equipment. **Figure 1** shows an example of the experimental setup used in the lab.

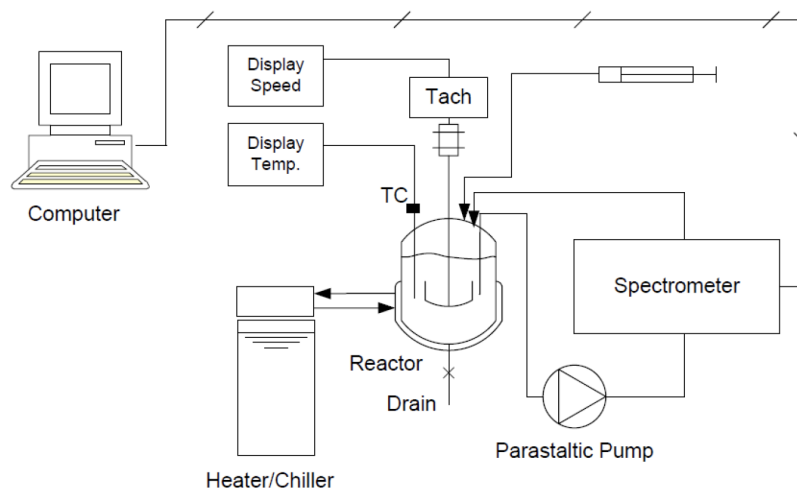


Figure 1: Schematic diagram of the experimental setup.¹

A one liter jacketed reactor would be used to house the iodination reaction. In order to keep the system within the desired temperature range, the jacket would be attached to a circulating bath. From there the temperature would be monitored with the digital display to show the user the thermocouple data. The thermocouple would be held in one of three injection ports located at the top of the reactor. Another of the three ports will be used for connection to the pump, while the last is used as the actual injection site for solutions. The peristaltic pump works to move a reactor volume to the UV spectrometer which then measures light absorbance in order to determine analyses based on their absorbance properties.

2.2. Materials

Hydrochloric acid, acetone, and iodine all have very serious hazards to be considered. HCl being corrosive and toxic, must be handled with care at all times. Acetone has a flash point of -20°C and for that reason must be stored and sealed carefully. Iodine requires the use of neoprene gloves as it can permeate through other glove materials. All are considered fairly serious health risks, and inhalation is a danger for all chemicals being used.

2.3. Safety Hazards

When performing this experiment, safety should be a crucial consideration. First and foremost at all times proper personal protective equipment should be worn. Splash goggles, a lab coat, and neoprene gloves must be worn while in the lab. Refer to **Appendix A** for a more clear description of chemical hazards associated with each reactant used in the lab. Material safety data sheets summarized in **Appendix A** show the chemicals in this lab may cause respiratory damage and should be handled under a

fume hood. Due to acetone's low flash point all sources of ignition should be removed from the lab to avoid fire. Needles must be disposed of in the proper containers, liquid waste in the liquid waste container, and the waste port should be sealed when finished.

2.4. Procedure

After safety considerations are made, the pump, circulator and spectrophotometer should be switched on. A designated amount of deionized water should be measured, while the temperature should be set along the agitation level. First inject water, then the acetone amount desired. As the system approaches the reaction temperature, inject HCl to calibrate the spectrophotometer. Drain the waste to appropriate containers once calibration is complete, and once cleaned the procedure may be repeated a desired amount of times, adding desired amounts of each chemical.

As previously mentioned, this experiment is conducted online, where the experimental data could be obtained via simulations in MATLAB. The P-Code used requires a set of conditions for each run of experiment as inputs, and the conditions associated with each run is summarized in **Table 1**.

Table 1: Initial conditions of different runs for data simulations.

Run	T (°C)	[CH ₃ COCH ₃] ₀ (M)	[HCl] ₀ (M)	[I ₂] ₀ (M)	Time (s)
1	35	2	0.02	0.0020	180
2	35	1	0.02	0.0020	180
3	35	3	0.02	0.0020	180
4	35	4	0.02	0.0020	180
5	35	2	0.01	0.0020	180
6	35	2	0.03	0.0020	180
7	35	2	0.04	0.0020	180
8	35	2	0.02	0.0010	180
9	35	2	0.02	0.0030	180
10	35	2	0.02	0.0040	180
11	30	2	0.02	0.0020	180
12	33	2	0.02	0.0020	180
13	40	2	0.02	0.0020	180
14	38	2	0.02	0.0020	180

Mathematical procedure of solving the desired parameters are described thoroughly in their own sections of the report, which are **Section 3** and **4**.

3. Results And Discussion

3.1. Determination of Reactions Orders α , β , and γ

Absorbance over time data alongside a calibration curve were simulated using the given MATLAB P-Code. Concentration over time data was then obtained by using **Eq. 4** which relates absorbance to concentration.

$$\text{Absorbance} = 96.654[I_2] + 0.0476 \quad \text{Eq. 4}$$

The rate law equation, **Eq. 1**, can be linearized with respect to α , β , and γ yielding **Eq. 5**, where the reaction rate can be considered $\frac{d[I_2]}{dt}$, the rate of iodine consumption.

$$\ln r_0 = \ln k + \alpha \cdot \ln[\text{Acetone}] + \beta \cdot \ln[\text{HCl}] + \gamma \cdot \ln[I_2] \quad \text{Eq. 5}$$

The method of initial rates is used to determine the rate order of each species. This method requires the calculation of the instantaneous rate of reaction at the very beginning of the experiment, as at this point the concentrations of the species can be approximated as their initial values. The concentration of each reagent, one at a time, is modified for each run while the other concentrations and temperature remain constant. This allows for the effect of each reagent on the reaction rate to be determined and thus the rate order. 10 simulations were conducted with three varied concentration runs for each of the three reagents and one standard run to compare to for a fixed temperature value, and another 4 simulations are performed for considering the variation in temperature.

Reaction rate is determined by finding the slope of the steep area in concentration over time simulated by the MATLAB P-Code, by only considering 1-10% of the first few data points to be linearized for each run. The rate order for each reaction is then determined by completing multiple linear regressions using Microsoft Excel's ANOVA function in its Data Analysis tool. The below **Table 2** details the rate order of each reagent along with the 95% confidence interval, standard error, and p-values associated with them.

Table 2: Rate orders with respect to each reactant with associated errors and p-values.

Parameter	Values	95% C.I.	Standard Errors	p-values
α	0.99	0.41 — 1.56	0.02	-
β	1.00	0.42 — 1.58	0.02	-
γ	-0.0003	-0.5774 — 0.5768	-0.0001	0.9990

The later **Section 3.3** below examines the uncertainty analysis in greater depth. The rate order values determined are very similar to the values found from the theoretical derivation as discussed in **Section 1**, $\alpha = 1$, $\beta = 1$, and $\gamma = 0$, with there being slight variation in the values determined by the simulations.

3.2. Determination of Arrhenius Parameters A and E_a

To determine the Arrhenius parameters A and E_a , five simulations were conducted using the MATLAB P-Code. One was the standard run used above and the remaining four runs had varied temperature while concentrations remained constant. Using the rate orders determined previously in **Table 2**, the method of initial rates and the linearized rate equation **Eq. 5**, k for each temperature could be determined. The run conditions and the corresponding k values are detailed in **Appendix B** alongside the standard error associated with the calculated rate constant.

With the rate constants determined for each temperature, the linearized Arrhenius equation, **Eq. 6**, can be used to determine values for E_a and A by using Microsoft Excel's ANOVA function in the Data Analysis tool to do multiple linear regressions for the data simulated.

$$\ln k = -\frac{E_a}{R} \cdot \frac{1}{T} + \ln A \quad \text{Eq. 6}$$

A is calculated by taking the exponential of the y-intercept calculated by the ANOVA function while the activation energy can be calculated by multiplying the determined slope by a factor of $-R$. The final values for A and E_a are shown below in **Table 3** with the 95% confidence intervals.

Table 3: Arrhenius parameters from the predetermined rate orders.

Parameter (Unit)	Values	95% C.I.
E_a (kJ · mol ⁻¹)	83.01	69.81 — 96.21
A (M ⁻¹ s ⁻¹)	1.03x10 ¹¹	5.95x10 ⁸ — 1.77x10 ¹³

A sample calculation to determine all these parameters tabulated above is as provided in **Appendix B**. Comparing the values obtained above to literature values of $E_a = 67.86$ kJ·mol⁻¹ and $A = 5.53 \times 10^7$ M⁻¹s⁻¹, a slight deviation could be seen from the values but a similar order of magnitude is noted.² The difference between the predicted values is most likely due to the different initial conditions used in the experiment done in literature, as they used a larger temperature range, from 35°C - 50°C, and smaller concentrations for acetone, and hydrochloric acid, which is 0.4 M and 0.2 M respectively. These differences in initial conditions will be propagated throughout the experiment to inevitably cause the slight deviation noted for E_a and A .

3.3. Uncertainty Analyses

Errors associated with measurement equipment lead to uncertainties in the measured values of absorbance, temperature, and mass. These uncertainties are ± 0.001 for absorbance, $\pm 0.1^\circ\text{C}$ for temperature, and ± 0.01 g for mass. Due to these measurements being the basis for the calculation of all further values, the error associated with them propagates leading to uncertainty associated with α , β , γ , k , A , and E_a . In addition to the manually propagated error analysis, 95% confidence intervals can also be determined to give an accurate range of plausible values for the calculated parameters. Furthermore, a sensitivity analysis on the volume of the reactor required to perform the reaction are conducted in **Appendix C** when α , β , γ , A , and E_a vary from the calculated values, at the same, considering the variations in initial conditions, including, T , q , k_2 , and initial concentrations of each reactant.

As discussed in the previous section, the determination of the E_a and A required a linear regression to be conducted. The linear regression itself along with the values for $\ln k$ and $1/T$ have errors associated with them and based on this, a 95% confidence interval can be calculated using **Eq. 7** seen below.

$$\text{Conf. Interval} = SE \text{ in } Y \text{ for each } X \cdot \sqrt{\frac{1}{n} + \frac{(x-\bar{x})^2}{\sum_i \sigma_x^2}} \quad \text{Eq. 7}$$

In **Eq. 7**, y values are associated with $\ln k$ and x values are associated with $1/T$ as this is the linearized form of the Arrhenius equation. The first term in **Eq. 7** is the standard error in $\ln k$ for each value of $1/T$ that is used to calculate it. In the square root, the denominator of the second term is the equation for the sum of squared deviations in $1/T$, while the numerator is the difference between $1/T$ and the average $1/T$ value squared. The calculated 95% confidence band is plotted around the regression result alongside the data points for simulated **Runs 11 - 14** with the associated error bars below in **Figure 2**.

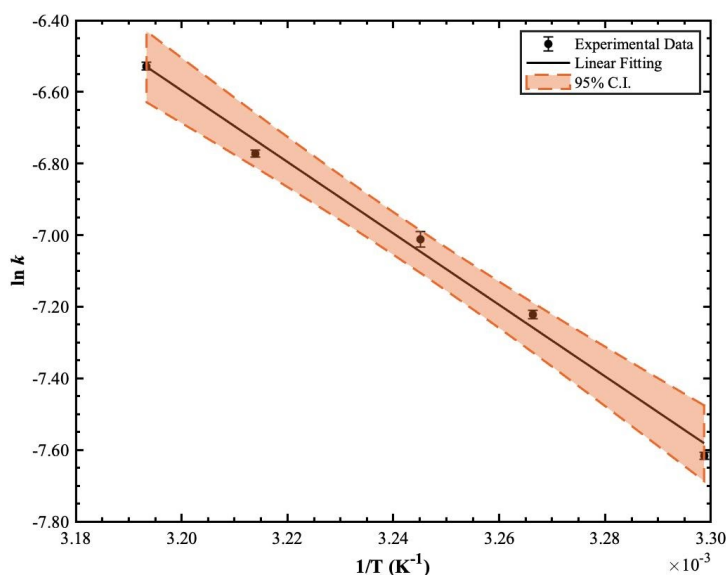


Figure 2: 95% confidence interval band for Arrhenius equation linearization for Run 11 - 14 data points.

Manual error propagation was also conducted to determine the direct error associated with each parameter in addition to the confident intervals determined above. The results of this work is seen below in **Table 4** where each parameter value is displayed with it's error and percent error propagate from experimental uncertainties.

Table 4: Determined parameters with their respective errors.

Parameter	Value	Error	Percent Error (%)
α	0.99	0.02	2.1
β	1.00	0.02	1.9
γ	-0.0003	-0.0001	22.8
$k (M^{-1}s^{-1})$	8.34×10^{-4}	4.55×10^{-6}	0.6
$E_a (kJ \cdot mol^{-1})$	83.01	7.07	8.5
$A (M^{-1}s^{-1})$	1.03×10^{11}	1.41×10^{10}	13.8

Notably γ has significantly larger error than the rest of the parameters and this is most likely due to the smaller absolute value of γ when compared to the other parameters causing the propagated error to be more prevalent in its determination.

The first error to be propagated was when the absorbance data and its error were used to calculate the concentration of iodine. This relationship is seen above in **Eq. 4** and the error was propagated through to the concentration value using **Eq. 8** for addition and subtraction and **Eq. 9** for multiplication and division.

$$\sigma_x = \sqrt{\sigma_a^2 + \sigma_b^2 + \sigma_c^2} \quad \text{Eq. 8}$$

$$\frac{\sigma_x}{x} = \sqrt{\frac{\sigma_a^2}{a^2} + \frac{\sigma_b^2}{b^2} + \frac{\sigma_c^2}{c^2}} \quad \text{Eq. 9}$$

Despite not measuring these results in person using a scale to maintain the most accurate assessment of the data, the error associated with mass measurements, ± 0.01 g, is propagated with the error of the concentration value. That error is then propagated through the calculation of the reaction rate. This is due to the reaction rate being calculated using a linear regression of concentration vs. time values. All of these errors are propagated out according to **Eq. 8** and **9**. Next, the rates were used in the method of initial reaction rates to determine α , β , and γ where the error associated with the rates are propagated to each of these parameters as well. As seen in the rate expression above **Eq. 1**, the parameters α , β , and γ are exponents and therefore will need to be calculated using the natural log. Error propagation from exponentials and logarithms is stated below in **Eq. 10** and was used to propagate the error from the rates to the error in each calculated rate order.

$$\frac{\sigma_x}{x} = y\left(\frac{\sigma_a}{a}\right) \quad \text{Eq. 10}$$

Furthermore, due to there being multiple runs used to determine each rate order, the final value is the average between these runs and the error of each individual calculation is propagated to the final value according to **Eq. 8** and **9**. By rearranging the rate expression in **Eq. 1**, k can be calculated as it is the only unknown in the equation now. Error will be propagated to this value as it is associated with the rate of reaction, concentration of reagents, and in the rate orders for each reagent. The error will be propagated according to **Eq. 8** and **9**. All parameters in the rate expression are now defined along with the error associated with them and as such the values for the activation energy and pre-exponential factors and their error can be determined using the Arrhenius equation. A linear regression is used to find the slope and y-intercept of the linearized Arrhenius equation which has error associated with it in addition to the error already associated with the rate constant and temperature values. These errors were propagated through the use of the above **Eq. 8 - 10** leading to the error in the calculated values for E_a and A .

4. Application Of Rate Law

The rate orders with respect to each reactant, activation energy, and pre exponential factor determined from the previous section are used in further analysis of reactor design and modelling. A common phenomenon could be observed in a reactor known as autocatalytic behavior, which leads to problems in system controls. This catalytic behavior arises due to the concentration of protons generated from the reaction approaches the initial concentration of protons from HCl. This behavior should be considered in further analysis moving forward to model the reactor and reaction more accurately.

4.1. Analysis of the Autocatalytic Regime in BSTR

Firstly a BSTR is used to model the reaction with the autocatalytic behavior. This could be modelled in MATLAB by comparing the concentration profile of the reactant. The ode function is used by employing the differential equations as shown in **Eq. 11**, with the initial conditions as listed in **Table 5**.

$$\frac{d[CH_3COCH_3]}{dt} = \frac{d[I_2]}{dt} = -\frac{d[HCl]}{dt} = -k_1[CH_3COCH_3]^\alpha[HCl]^\beta[I_2]^\gamma \quad \text{Eq. 11}$$

Table 5: Initial conditions to model autocatalytic behavior in BSTR.

Parameters	Values (Units)
$[CH_3COCH_3]_0$	2.000 M
$[HCl]_0$	0.001 M
$[I_2]_0$	0.010 M
Temperature	303 K
Time Frame	5000 s

The concentration profile of acetone and protons are as shown in **Figure 3** and **4** over a time frame of 5000 s respectively.

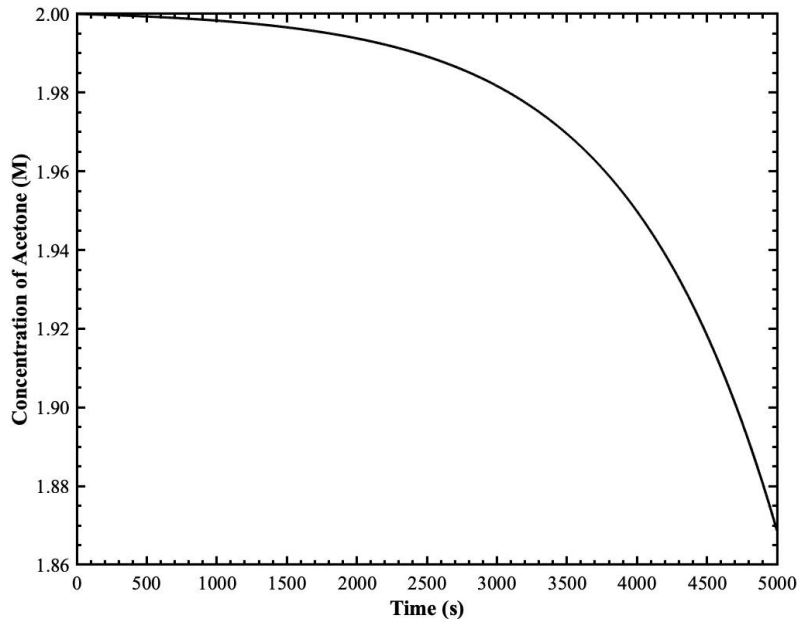


Figure 3: Predicted data of acetone concentration in a batch reactor.

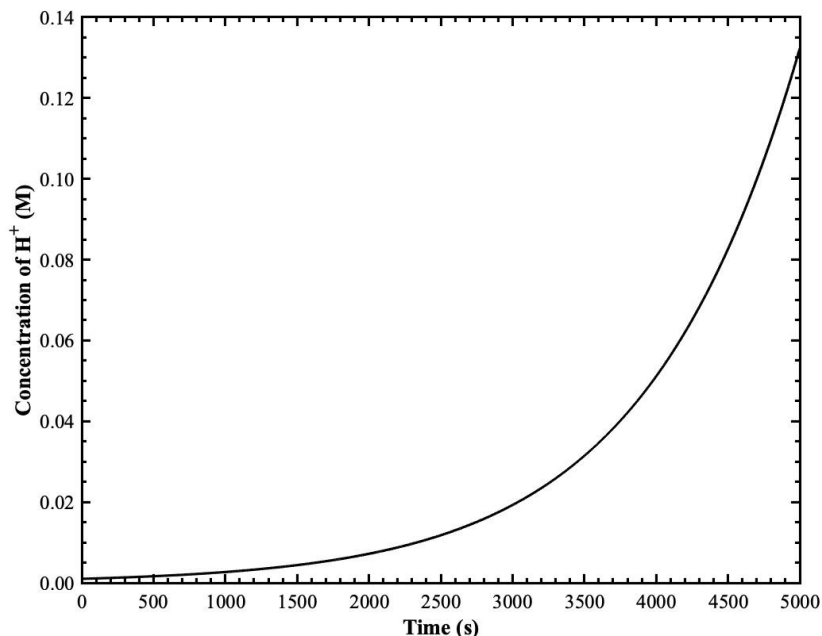


Figure 4: Predicted data of proton concentration in a batch reactor.

From **Figure 3**, it could be seen that the concentration of acetone decreases with time, while protons are generated at the same time as illustrated in **Figure 4**. A comparison of I_2 concentration changes with time predicted by the modelling of **Eq. 11** and as simulated from the P-Code was done, and as plotted in **Figure 5**.

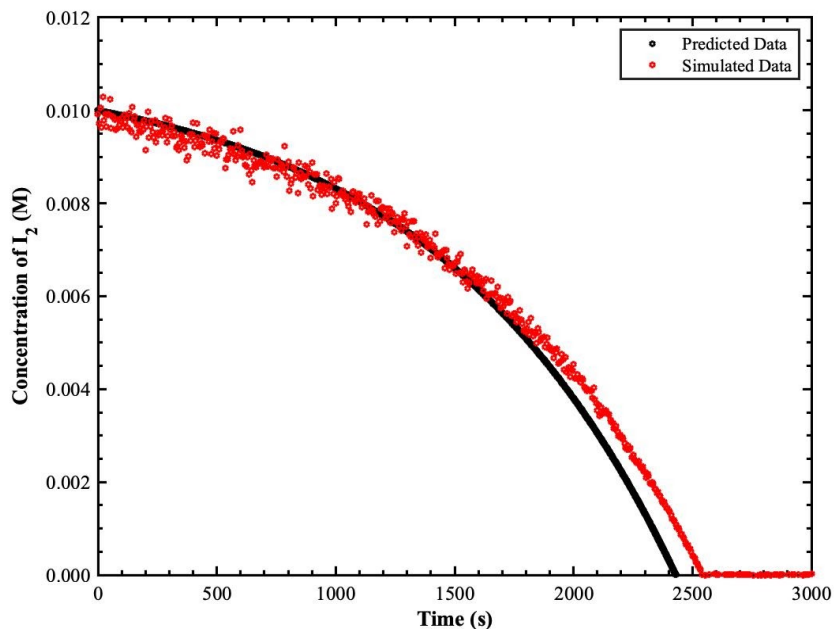


Figure 5: Predicted and simulated data of I_2 concentration in a batch reactor.

From **Figure 5**, the proposed model closely predicted the concentration profile of I_2 to that of the simulation data. After approximately 2500s of reacting, the concentration reaches unity at 0 M. Data beyond 3000s were not shown as the values just plateaued at 0 M and are irrelevant.

4.2. Analysis of Acetone Iodination in Conjunction with HI electrolysis

To avoid the autocatalytic behavior in the reactor, the concentration of protons could be reduced by performing electrolysis on HI, which is the side product of the main reaction to form hydrogen and iodine gas. The reaction could be written as shown in **Rxn. 5**, with the rate of hydrogen production as shown in **Eq. 12**.



$$r_{H_2, +} = k_2[I^-], \quad k_2 = 0.081s^{-1} \quad \text{Eq. 12}$$

With the addition of a second reaction, the differential equations from **Eq. 11** should be modified to as listed below in **Eq. 13 - 16**, alongside the consideration of change in iodide ion concentration in the system as shown in **Eq. 16**.

$$\frac{d[CH_3COCH_3]}{dt} = -k_1[CH_3COCH_3]^\alpha[HCl]^\beta[I_2]^\gamma \quad \text{Eq. 13}$$

$$\frac{d[HCl]}{dt} = k_1[CH_3COCH_3]^\alpha[HCl]^\beta[I_2]^\gamma - 2k_2[I^-] \quad \text{Eq. 14}$$

$$\frac{d[I_2]}{dt} = -k_1[CH_3COCH_3]^\alpha[HCl]^\beta[I_2]^\gamma + k_2[I^-] \quad \text{Eq. 15}$$

$$\frac{d[I^-]}{dt} = k_1[CH_3COCH_3]^\alpha[HCl]^\beta[I_2]^\gamma - 2k_2[I^-] \quad \text{Eq. 16}$$

Using the initial conditions from **Table 5**, the concentration profile of acetone and proton could be determined, as plotted in **Figure 6** and **7** respectively.

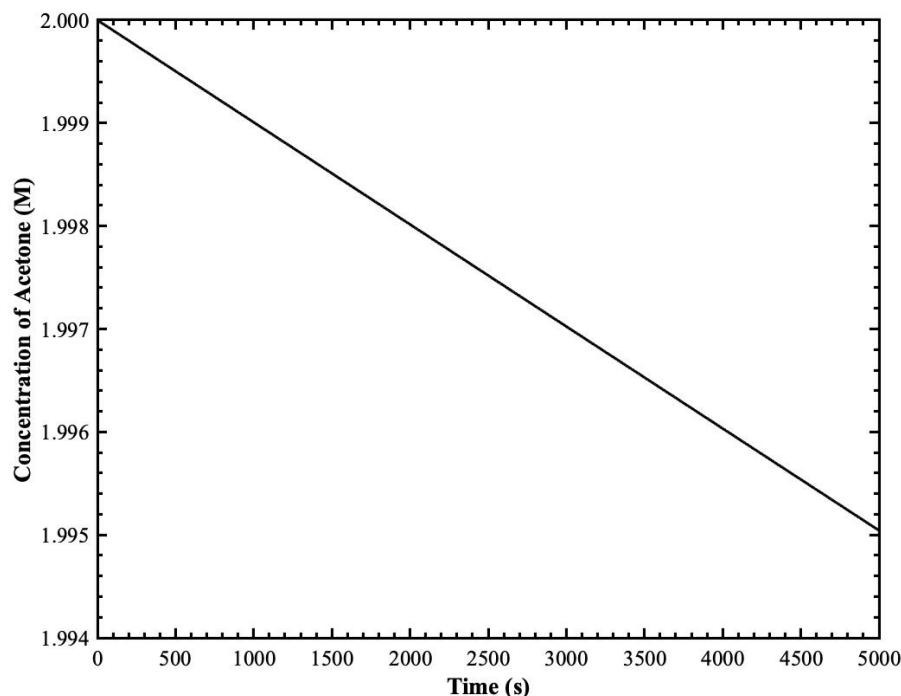


Figure 6: Predicted data of acetone concentration in a batch reactor with HI electrolysis.

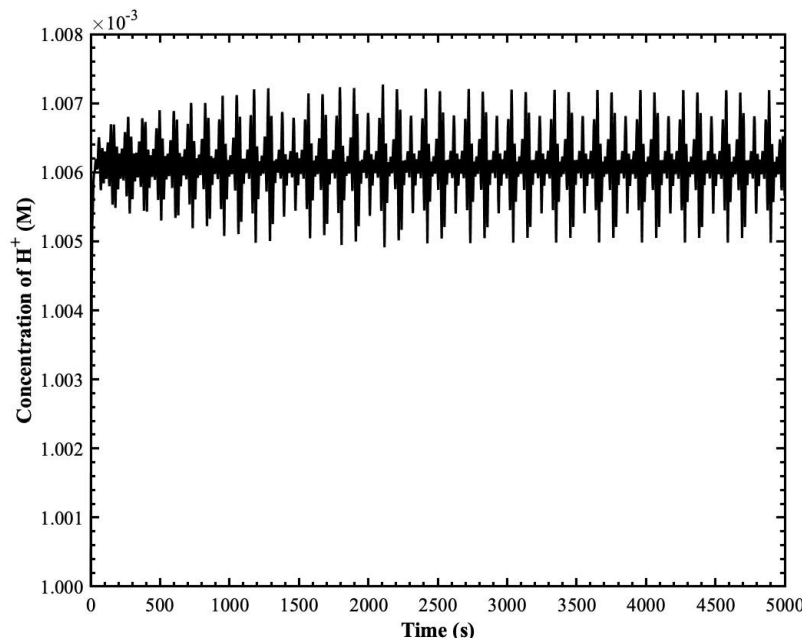


Figure 7: Predicted data of proton concentration in a batch reactor with HI electrolysis.

Over a time frame of 5000 s, the concentration of acetone decreased linearly in **Figure 6**, as opposed to the previous analysis in **Section 4.1 (Figure 3)**. It is also observed that the concentration is slightly greater over time. Electrolysis reaction is reacting and competing with the main reaction, which slows down the consumption of acetone to form the products. From **Figure 7**, it is noted that instead of increasing over time as observed from the previous section (**Figure 4**), proton concentration fluctuates over time around 1.006×10^{-3} M. This is expected as protons are generated in the first reaction but then consumed in the second reaction to form hydrogen and iodine gas. The kinetics for both reactions are quite similar in a way that the fluctuations did not vary a lot from time to time. Next, the concentration profile of I_2 of the predicted vs. the simulated data are as illustrated in **Figure 8**.

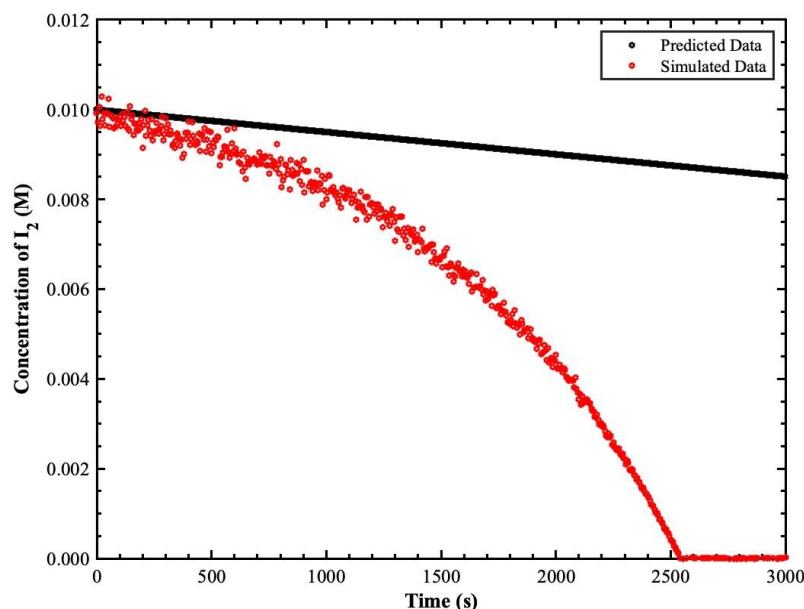


Figure 8: Predicted and simulated data of I_2 concentration in a batch reactor with HI electrolysis.

It is apparent that the concentration of I_2 did not reach 0 over time as seen from the previous section as expected. I_2 is initially consumed by the first reaction, but immediately produced in the second reaction. As per simulated data, I_2 is no longer present in the reactor at approximately 2500s as it did not take the second reaction mechanism into account. The acceleration of I_2 consumption goes hand in hand with the autocatalytic behavior, which is no longer observed when employing the electrolysis reaction in the reactor.

4.3. CSTR Sizing

Analysis on a CSTR is done next. An appropriate scaling of reactor volume is needed for a pilot facility. It is of interest to produce iodoacetone by using the electrolysis strategy as thoroughly discussed in the previous section for improved reactor stability and efficiency. The electrolysis reaction is the same as shown in **Rxn. 5**, but with a modified reaction rate of hydrogen formation, as written in **Eq. 17**.

$$r_{H_2, +} = k_2[I^-], k_2 = 0.53 L \cdot s^{-1} \quad \text{Eq. 17}$$

To model the concentration profile of reactants and products in CSTR, a new set of differential equations should be proposed. As of CSTR, a few assumptions can be made to simplify the differential equations for further analyses. Due to the liquid phase of all reactants, there is little to no volumetric change in inflow and outflow that could be assumed to be constant. Plus, the reactions can be modeled as a steady-state operation. By employing these assumptions, the mole balances of each compound could be used to solve for the CSTR sizing, from the basis of **Eq. 18**, and **Eq. 19 - 22** will be the mole balance for each compound.

$$\frac{dn_i}{dt} = 0 = q([i]_0 - [i]) + rV \quad \text{Eq. 18}$$

$$\frac{dn_{CH_3COCH_3}}{dt} = 0 = q([CH_3COCH_3]_0 - [CH_3COCH_3]) - k_1[CH_3COCH_3]^\alpha[HCl]^\beta[I_2]^\gamma V \quad \text{Eq. 19}$$

$$\frac{dn_{HCl}}{dt} = 0 = q([HCl]_0 - [HCl]) + k_1[CH_3COCH_3]^\alpha[HCl]^\beta[I_2]^\gamma V - 2k_2[I^-] \quad \text{Eq. 20}$$

$$\frac{dn_{I_2}}{dt} = 0 = q([I_2]_0 - [I_2]) - k_1[CH_3COCH_3]^\alpha[HCl]^\beta[I_2]^\gamma V + k_2[I^-] \quad \text{Eq. 21}$$

$$\frac{dn_{I^-}}{dt} = 0 = q([I^-]_0 - [I^-]) + k_1[CH_3COCH_3]^\alpha[HCl]^\beta[I_2]^\gamma V - 2k_2[I^-] \quad \text{Eq. 22}$$

A new set of initial conditions and constraints are as tabulated in **Table 6**, with a fixed conversion of acetone to be used to solve for its final concentration, as shown in **Eq. 23**.

Table 6: Initial conditions for the CSTR sizing.

Parameters	Values (Units)
χ	80 %
q	$10 L \cdot min^{-1}$
Temperature	353 K
$[CH_3COCH_3]_0$	2.000 M
$[HCl]_0$	0.001 M
$[I_2]_0$	1.000 M

$$[CH_3COCH_3] = (1 - \chi)[CH_3COCH_3]_0 \quad \text{Eq. 23}$$

A system of equations with four equations and variables could be solved simultaneously and is done in MATLAB. The final values of the reactants' concentrations and sizing of the CSTR volume are as tabulated below in **Table 7**.

Table 7: Final prediction of concentration and CSTR volume sizing.

Parameters	Values (Units)
$[CH_3COCH_3]$	0.4000 M
$[HCl]$	0.2184 M
$[I_2]$	0.0913 M
$[I^-]$	0.2174 M
V	56.6 ± 4.9 L (90% C.I.)

It was found that the required CSTR volume is 56.62 L. The volume is reasonable for a small number of reactions and a shorter desired time frame to observe the entire reaction. The volume was determined to vary ± 4.92 L based on the 90 % confidence interval. It is important to consider these volume variations in order to build a reactor that can still meet the desired requirements, at the same time, spending less capital in setting up the reactor volume.

5. Conclusions And Recommendations

5.1. Conclusions

MATLAB P-Code was used to run a series of simulations for the iodination of acetone reaction to determine the rate order for each reagent, rate constant, pre-exponential factor and activation energy. Using the method of initial rates for the simulated data, the rate orders α , β , and γ were calculated to be 0.99 ± 0.02 , 1.00 ± 0.02 , and -0.0003 ± 0.0001 respectively. Using these calculated orders, further analysis was conducted leading to use of the Arrhenius equation to determine the activation energy and pre-exponential factor, and were determined to be 83.01 ± 7.07 kJ·mol⁻¹ and $1.03 \times 10^{11} \pm 1.41 \times 10^{10}$ M⁻¹s⁻¹ respectively. Error was propagated throughout the determined values to account for the random error in the system and any error associated with measurement data. MATLAB and Excel sheets used are provided in **Appendix D**.

The values determined in this experiment are then further used to analyze this reaction system when completed in a BSTR and a CSTR. A system of ODEs was constructed to model the concentrations of the various species in this reaction. Analyzing the BSTR at first, an autocatalytic behavior is noted which can cause problems in the system controls and is therefore avoided in the next set of simulations by the use of HI electrolysis. This electrolysis model showed a linear decrease in acetone and iodine concentration rather than the parabolic relationship shown with the electrolysis which caused the reaction time to be slower due to the electrolysis reaction competing with the main reaction. Examining this reaction using a CSTR, the required volume to obtain acetone conversion of 80% with a volumetric flow rate of 10 L·min⁻¹ was determined to be 56.6 ± 4.9 L.

5.2. Recommendations

When conducting this experiment, there are two steps that need to be understood to a high degree of detail to have success. First is to completely understand the experiment and all relevant safety aspects such as the special hazards associated with steps, required personal protection equipment, and each chemical safety data sheet. To achieve the highest accuracy with the data produced, the inherent errors in measurement equipment need to be propagated through thoroughly. This analysis is crucial as it gives an accurate band of possible values for the determined data to a high confidence value.

Due to the virtual nature of this investigation, the potential modifications to experimental procedure are limited. The first modification could only occur with the ability to conduct experiments in person, and would have the hydrogen iodine electrolysis experiments to compare real data to the autocatalytic reaction. In the simulated environment, a modification to the procedure would be to simulate the imprecision of mass measurements that would occur in the lab experiment.

6. Nomenclature Table

Table 8: Summary of nomenclatures and abbreviations used throughout the report.

Variables	Definition
α	Rate order with respect to acetone
β	Rate order with respect to hydrochloric acid
γ	Rate order with respect to iodine gas
k	Rate constant ($\text{M}^{-1}\text{s}^{-1}$)
σ_x	Error propagated of variable x
τ	Residence time (s or min)
χ	Conversion
n_i	Mole of species i (mol)
r_0	Initial rate of reaction ($\text{M}\cdot\text{s}^{-1}$)
q	Volumetric flow rate ($\text{L}\cdot\text{min}^{-1}$)
ϵ	Molar absorptivity ($\text{M}^{-1}\text{cm}^{-1}$)
b	Length for light passes through the absorption (cm)
T	Temperature (K or $^{\circ}\text{C}$)
E_a	Activation energy ($\text{J}\cdot\text{mol}^{-1}$ or $\text{kJ}\cdot\text{mol}^{-1}$)
A	Pre-exponential factor ($\text{M}^{-1}\text{s}^{-1}$)
R	Gas constant ($8.314 \text{ J}\cdot\text{mol}^{-1}\text{K}^{-1}$)
V	Volume of reactor (L)
$[i]$	Molarity of species i
CH_3COCH_3	Acetone
HCl	Hydrochloric acid
I_2	Iodine gas
I^-	Iodide ions
HI	Hydrogen iodide gas
H_2	Hydrogen gas
BSTR	Batch stirred tank reactor
CSTR	Continuous stirred tank reactor

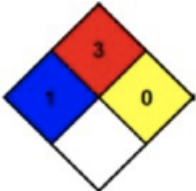

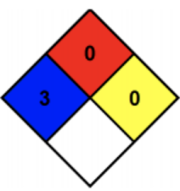
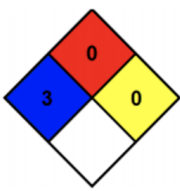
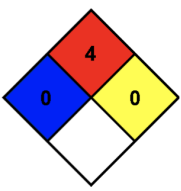
7. References

- ¹ Orazov, M. CHEG 345 Kinetics Experiment. Chemical Engineering Laboratory I: CHEG 345. University of Delaware.
- ² Yao, X.; Deng, Q.; Wang, S.; Wang, W.; Hou, Y. I.; Gao, Z.; Wu, Y.; Guo, Z. Acetone Iodination Kinetics in Flow with Online UV Monitoring and Continuous Control. *ChemistrySelect* 2019, 4 (17), 5116–5121.
- ³ Acetone; CAS No. 67-64-1 [Online]; LabChem, Inc; Zelienople, PA, November 12, 1998. <https://www.labchem.com/tools/msds/msds/LC10420.pdf> (accessed 4/14/21).
- ⁴ Hydrochloric Acid; CAS No. 7647-01-0 [Online]; LabChem, Inc; Zelienople, PA, July 3, 2013. <https://www.labchem.com/tools/msds/msds/LC15300.pdf> (accessed 4/14/21).
- ⁵ Iodine; CAS No. 7553-56-2 [Online]; LabChem, Inc; Zelienople, PA, November 4, 2003. <http://www.labchem.com/tools/msds/msds/LC15590.pdf> (accessed 4/14/21).
- ⁶ Hydrogen Iodide; CAS No. 10034-85-2 [Online]; Matheson Tri-Gas, Inc; Basking Ridge, NJ, March 7, 1990. <https://www.mathesongas.com/pdfs/msds/MAT11100.pdf> (accessed 4/14/21).
- ⁷ Hydrogen; CAS No. 1333-74-0 [Online]; Praxair, Inc; Danbury CT, January 1, 1980. <https://isolab.ess.washington.edu/safety/sds/hydrogen.pdf> (accessed 5/10/21).

8. Appendices

Appendix A: Chemical Properties And Safety Hazards

Table A1: Summary of safety hazards and protective measures of the reactants/products involved.

Properties	CH_3COCH_3 ³	HCl ⁴	I_2 ⁵	HI ⁶	H_2 ⁷
NFPA Diamond					
NIOSH REL (ppm)	250	5	0.1	N/A	N/A
Stability and reactivity	Violent to explosive reaction.	Thermal decomposition generates corrosive vapor.	Thermal decomposition generates corrosive vapor.	Containers may rupture if exposed to heat.	Can form explosive mixtures with air.
Special protective measures	Full face mask with filter type AX at concentration in air greater than exposure limit.	Nothing specific to HCl.	Gas masks are required.	Respiratory protection is needed.	Consider the use of flame resistant anti-static safety clothing.

Appendix B: Sample Calculations

The P-Code is used to obtain the simulated absorbance data of iodine for all runs tabulated in **Table 1** as shown in **Figure B1**.

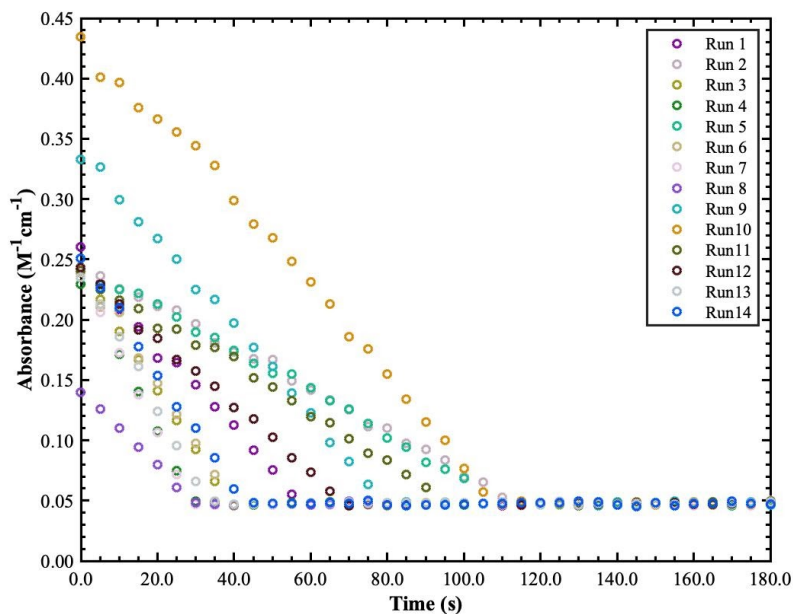


Figure B1: Absorbance data varying with time for all run conditions.

From this absorbance data, the associated iodine concentration could be determined based on **Eq. 4**. Iodine concentration varies with time and a linear fitting should be done on approximately 1-10% of the first few data points. This is done in such a manner to depict the initial rate of reaction for each run, as the initial rate method is pursued to determine the rate order with respect to each reactant. The concentration of iodine decreases with time, as shown in **Figure B2a**, with its linear fitting for each run in **Figure B2b**, and the initial reaction rate for each run is as tabulated in **Table B1**.

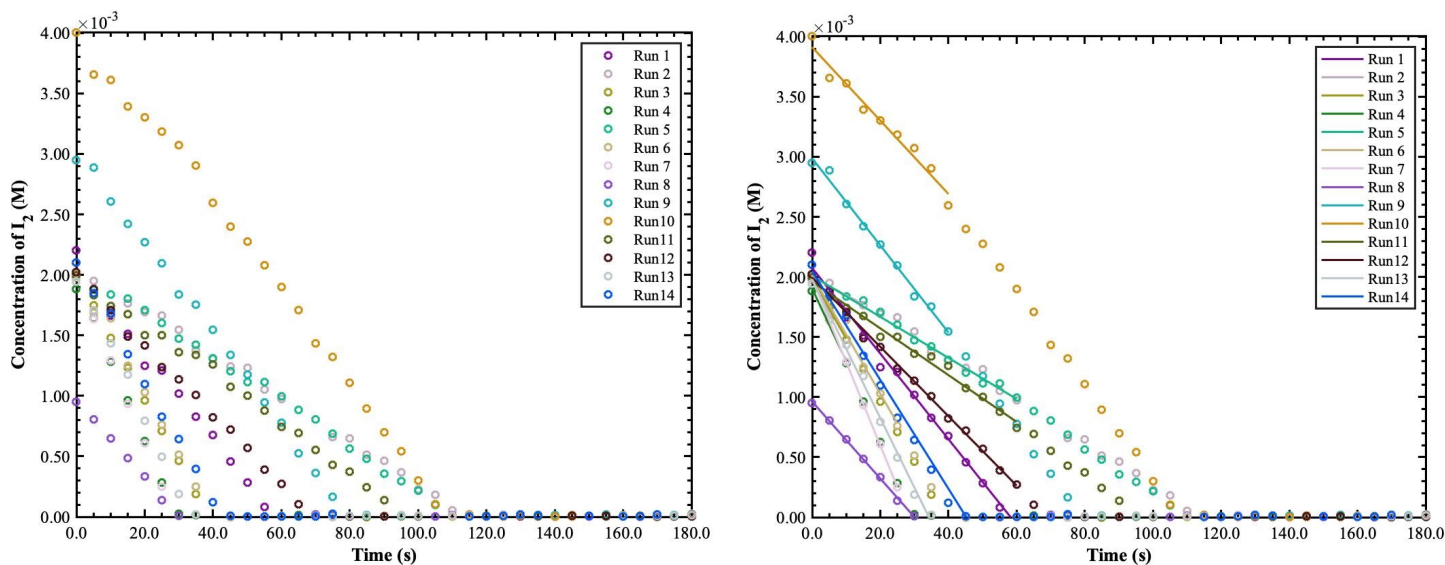


Figure B2: a) Concentration of I_2 varying with time (left) and b) linear fitting for initial rate of reaction determination (right) for each run.

Table B1: Initial rate of reaction for each run from linear fitting of the I₂ concentration profile.

Run	r ₀ (M·s ⁻¹)	[CH ₃ COCH ₃] ₀ (M)	[HCl] ₀ (M)	[I ₂] ₀ (M)	ln r ₀	ln [CH ₃ COCH ₃] ₀	ln [HCl] ₀	ln [I ₂] ₀
1	3.5604 x 10 ⁻⁵	2.000	0.020	0.0020	-10.2431	0.6931	-3.9120	-6.2146
2	1.5291 x 10 ⁻⁵	1.000	0.020	0.0020	-11.0882	0.0000	-3.9120	-6.2146
3	4.9796 x 10 ⁻⁵	3.000	0.020	0.0020	-9.9076	1.0986	-3.9120	-6.2146
4	6.0234 x 10 ⁻⁵	4.000	0.020	0.0020	-9.7173	1.3863	-3.9120	-6.2146
5	1.7092 x 10 ⁻⁵	2.000	0.010	0.0020	-10.9769	0.6931	-4.6052	-6.2146
6	4.9220 x 10 ⁻⁵	2.000	0.030	0.0020	-9.9192	0.6931	-3.5066	-6.2146
7	6.9323 x 10 ⁻⁵	2.000	0.040	0.0020	-9.5767	0.6931	-3.2189	-6.2146
8	3.2025 x 10 ⁻⁵	2.000	0.020	0.0010	-10.3490	0.6931	-3.9120	-6.9078
9	3.6251 x 10 ⁻⁵	2.000	0.020	0.0030	-10.2250	0.6931	-3.9120	-5.8091
10	3.0549 x 10 ⁻⁵	2.000	0.020	0.0040	-10.3962	0.6931	-3.9120	-5.5215
11	1.9456 x 10 ⁻⁵	2.000	0.020	0.0020	-10.8474	0.6931	-3.9120	-6.2146
12	2.8866 x 10 ⁻⁵	2.000	0.020	0.0020	-10.4529	0.6931	-3.9120	-6.2146
13	5.7767 x 10 ⁻⁵	2.000	0.020	0.0020	-9.7591	0.6931	-3.9120	-6.2146
14	4.5263 x 10 ⁻⁵	2.000	0.020	0.0020	-10.0030	0.6931	-3.9120	-6.2146

In the same table, the values of each term in the linearization equation of the initial rate law as demonstrated in **Eq. 5** are tabulated. Multiple linear regression (MLR) in Excel is performed to determine the rate order with respect to each reactant. The MLR outputs are as shown in **Table B2**.

Table B2: MLR outputs to determine rate order with respect to each reactant.

	Coefficients	Standard Error	t Stat	P-value	Lower 95%	Upper 95%
Intercept	-7.0739	1.9086	-3.7063	0.0041	-11.3266	-2.8213
ln [CH₃COCH₃]₀	0.9876	0.2590	3.8129	0.0034	0.4105	1.5647
ln [HCl]₀	1.0014	0.2590	3.8662	0.0031	0.4243	1.5785
ln [I₂]₀	-0.0003	0.2590	-0.0012	0.9990	-0.5774	0.5768

The orders for each reactant are listed in the coefficients column accordingly in **Table B2**. With these values, the rate constants for each run could be determined by rearranging the rate law from **Eq. 1**, as shown in **Eq. B1** below and are tabulated in **Table B3**.

$$k = \frac{r_0}{[\text{CH}_3\text{COCH}_3]^\alpha [\text{HCl}]^\beta [\text{I}_2]^\gamma} \quad \text{Eq. B1}$$

Table B3: Variations in rate constants for Arrhenius parameters determination.

Run	T (°C)	1/T (K ⁻¹)	k (M ⁻¹ s ⁻¹)	Standard Error in k (M ⁻¹ s ⁻¹)	ln k
1	35	0.003245	9.0023×10^{-4}	1.9135×10^{-5}	-7.0121
11	30	0.003299	4.9194×10^{-4}	4.6219×10^{-6}	-7.6164
12	33	0.003266	7.2986×10^{-4}	8.6087×10^{-6}	-7.2219
13	40	0.003193	1.4606×10^{-4}	1.6151×10^{-5}	-6.5281
14	38	0.003214	1.1445×10^{-4}	1.0993×10^{-5}	-6.7721

With these k values, the E_a and A values of the reactions could be determined. Only the runs with variations in temperature are considered for these determination, which would be **Run 1** and **11 - 14**. From this data, the linearization of Arrhenius equation (**Eq. 6**) was performed, and the relevant parameters are also tabulated in **Table B3**.

Appendix C: Supplemental Sensitivity Analysis Discussion

In Phase 3, it was required to determine the volume of CSTR based on the given set of initial conditions. In this section, thorough discussion was done on the sensitivity analysis of the computed volume based on the variations in the predicted parameters from Phase 1 and 2 (i.e. α , β , γ , E_a , and A) and the initial provided conditions (i.e. k_2 , T , q , $[\text{CH}_3\text{COCH}_3]_0$, $[\text{HCl}]_0$, $[\text{I}_2]_0$). This analysis is crucial and important as the changes in volume of the reactor directly reflects the amount of iodoacetone that could be produced at a given time for a particular set of conditions. **Figure C1** shows the effect of varying the predicted parameters on the changes in CSTR volumes.

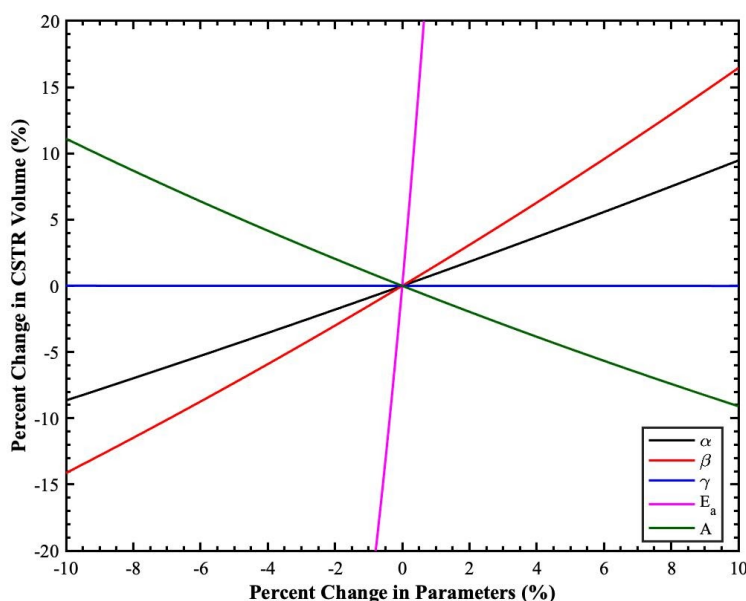


Figure C1: Changes in volume of CSTR after varying the predicted parameters from Phase 1 and 2.

From **Figure C1**, it could be seen that as the values of α , β , and E_a varied from 10% smaller to 10% greater than the actual values, the CSTR volume changes in the same direction, where it increases as the parameters' values increase. It is interesting to note that only a small change in E_a could increase the

volume of CSTR required in the reaction by a lot. This is expected as the activation energy determines the kinetics of the reactions. In other words, the reaction would be run longer if the activation energy is greater. When this is the case, a greater volume of reactor is needed to accommodate a longer reaction time for the same amount of product produced and the same initial conditions. On the other hand, α and β do not increase the volume by that much as that of E_a . This is associated with the order of acetone and HCl respectively. In principle, the reaction would be carried out in a smaller volume as the rate of reaction is greater when the order of reaction slightly increases while remaining the initial flow rate and concentration constant, if the concentration is greater than 1 M. However, this experiment is dealing with initial concentration that is less than 1 M, in which mathematically, will have a lower rate of reaction, leading to an increase in volume of the CSTR required to operate at the particular conditions. The volume does not increase in the same magnitude as changing E_a does because the orders were only varied within a value of 1, which is less significant when one tries to vary the order within the order of 2, 3, or any higher order.

On the other hand, when γ values were varied, there were little to no changes in volume. This is expected as the order of I_2 is close to 0 (in theory, it is exactly 0). It is very insignificant (which is proven by high p-value from 95% confidence interval analysis) that it will not affect the volume used in the reaction. However, it is expected to have a considerable effect of volume changes if γ were to be varied around a larger value, i.e. 2 or 3, though this would not be the case for this particular reaction. On the flip side, as the value of A increases, the volume of the reactor would decrease. The pre-exponential factors reflect the number of collisions of molecules that could happen in a given time interval. A greater factor would mean more molecules collided with each other to react and form the desired product. A is also related to the rate constant, in which increasing A would make the reaction run faster. In turn, a smaller volume of reactor is needed as the reaction is happening faster to produce the same amount of product.

Next, variations in initial provided conditions and their effects on the volume of the reactor are analyzed. **Figure C2** shows the changes in volume as the initial conditions varied ranging from values 10% smaller and greater than the actual values.

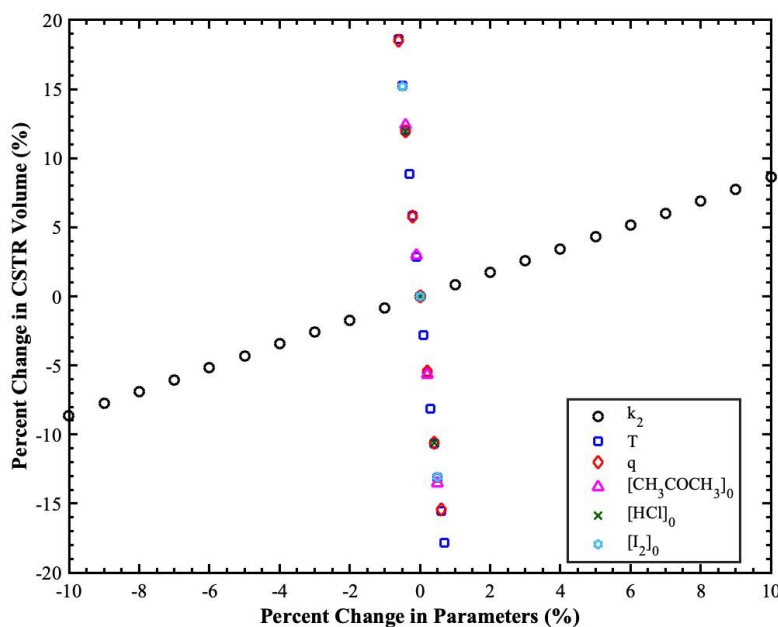


Figure C2: Changes in volume of CSTR after varying the provided initial parameters from Phase 3.

In consensus, varying T , q , and initial concentration of all reactants by only small values have a significant decrease in volume of the reactor. To understand the changes in volume for T variations, the Boltzmann curve should be consulted. Boltzmann predicted the number of particles with the energy greater than a particular E_a value when the temperature is increased. From here, it makes conceptual sense in requiring only a smaller volume of reactors as the molecules are now colliding more frequently with each other to form the same amount of product at a shorter time. Same goes to the increase in initial concentrations. When the reaction is started with a greater amount of reactants, by Le Chatelier's principle, the equilibrium will drive the reaction to produce more products. Hence, for a fixed amount of desired product, only a small reactor volume is needed. As of q , when more reactants are flowing into the reactor, smaller reactor volumes are required. In order to have the same conversion of acetone to iodoacetone, the residence time should remain constant. Due to that, as q increases, for a fixed value of τ , smaller volume is needed. In contrast, as the rate constant of the electrolysis, k_2 is increased, the volume of the reactor will increase too. As discussed in **Section 4** of the report, HI electrolysis is a competing reaction with the main reaction. Reducing HI at a greater rate would imply reducing the concentration of protons in the reactor a lot faster than it is being produced by the main reaction. Because of this, a greater volume would be needed to accommodate this faster second reaction in order to achieve the same amount of production.

Appendix D: MATLAB Code and Excel Sheet

- The file to MATLAB Code for generating all figures and Excel Sheet for the calculations can be accessed through [here](#).